Indian Journal of Pure & Applied Physics
Vol. 61, May 2023, pp. 309-325
DOI: 10.56042/ijpap.v61i5.71257

Performance Evaluation of GPU-Based WRF Model in Simulating a Unique Tropical Cyclone of Arabian Sea: A Case Study of VSCS Vayu

Pubali Mukherjee* & Balaji Ramakrishnan

Department of Civil Engineering, Indian Institute of Technology Bombay, Mumbai 400 076, India

Received 9 February 2023; accepted 13 April 2023

Tropical cyclone (TC) Vayu developed from a low-pressure system on 9 June 2019 near the West coast of India. It underwent rapid intensification (RI) to a very severe cyclonic storm (VSCS) before weakening into a deep depression on 17 June 2019 with a unique track. The present study aims to evaluate the performance of the GPU-WRF model in simulating the unique tropical cyclone Vayu when initialized with different meteorological boundary conditions and the effect of input of time-varying SST data, the track, and the cyclone's intensity. The study also aims to investigate the cyclone's synoptic parameters during its development and intensification. Four simulations are conducted with GFS and NCEP-FNL data with and without SST input. The four-dimensional data assimilation analysis technique, the fdda analysis nudging scheme, was used on the GFS data with SST input, which showed a significant improvement in track and intensity. The system skirting the Gujrat coastline on 13 June is skillfully captured. Given the appreciable improvement of track and intensity with GFS data using nudging, further investigation of the cyclone's synoptic parameters is done on the same. Overall, comparing the simulated dynamics with the ERA-5 dataset indicated that the model simulated a stronger TC. WRF can skillfully simulate a well-delineated eye wall at the matured stage (wind speed >40 m/s). An anomalously high mid-tropospheric relative humidity (RH) (~90%) is indicated at the developing stage, indicating the onset of RI, during which the system showed RH ~100% at the mid-troposphere. On 14 June, when the system reached VSCS, the simulated storm's low-level relative vorticity was ~359.93 × 10^{-5} s^{-1}, whereas ERA-5's was ~175.39 × 10^{-5} s^{-1}only.The simulated storm cyclone energy (9.35×10^4 $knts^2$) was lower than the observed (11.54×10^4 $knts^2$). The significance of the results obtained from the study is that the model can skillfully simulate the track and intensity of an Arabian Sea TC and capture TC Vayu's cyclogenesis. The study also provides insight into the cyclone's synoptic parameters, such as mid-tropospheric relative humidity, low-level relative vorticity, and cyclone energy, during its development and intensification. The study's findings can be useful in improving the accuracy of tropical cyclone forecasting and enhancing our understanding of the physical processes involved in their formation and intensification for the Arabian Sea region.

Keywords: WRF; GFS; NCEP; SST; Nudging; Cyclone Vayu; GPP

1 Introduction

The northern Indian Ocean has two significant tropical cyclone (TC) seasons, pre-monsoon and post-monsoon. TC Vayu is a pre-monsoon cyclone that originated from a low-pressure system in the Arabian Sea on 9 June 2019.Underfavourable environmental conditions, the system soon developed into a deep depression. Eventually, it underwent rapid intensification to a very severe cyclone (VSCS) on 11 June 2019, 18 UTC, centering itself over the eastern Arabian Sea. Until 13 June, this VSCS moved northwards towards the Gujarat coastline, recurving its path. Later, on 16 June, Vayu moved northeast, weakening into a cyclonic storm. Based on the numerical weather prediction model (NWP) forecast, the India Meteorological Department (IMD) predicted the probable landfall on 12 June along the Gujarat coastline. However, the system skirted the Gujrat coastline as a VSCS storm due to multiple interactions with the mid-latitude westerlies causing the system to move upwards, taking a unique track. The unique forecast track of VSCS Vayu with multiple recurving proved challenging for the IMD. Initial prediction by IMD led to the emergency evacuation of the coastal populations. Necessary hazard preparations were undertaken by the Government of India[1], as the Gujrat coastline is a high-risk zone among the hazard-prone districts[2].There have been continuous improvements in the TC intensity and track forecasts by IMD over the decade[3]. IMD's average track forecast error has improved from 123 km during the 2009-2013 period to 81 km during the 2014-2018 period for 24 hours forecasting by NWP models[1]. However, the track

*Corresponding author: (E-mail: pubalimukherjee362@gmail.com)

prediction of TC Vayu was a unique case, and it was a significant challenge for IMD. A comparative study on the HWRF model coupled with well-known ocean models by Das *et al*.[4] indicated a poor prediction of cyclone Vayu track. The study indicated a high positional error owing to the unique track of the storm with multiple recurring segments, even with a lead time of 2 days. Due to the modern data assimilation techniques, several advancements have been made in the track prediction of TC of the NIO, but there is still scope for development in terms of numerical simulations of intensity and track predictions. Especially in the dynamics of rapid intensification (RI)[5]. The Northern Indian Ocean (NIO) has witnessed the cyclogenesis of several devastating storms due to its typical warm climate[6], and WRF-ARW has been extensively used for the prediction of these TCs of the NIO since 2007[7]. Previous research has demonstrated the reliability of the WRF model in studying tropical cyclones (TCs) in the North Indian Ocean (NIO)[1,8–14]. The incorporation of the WRF model with storm surge and ocean models has resulted in successful surge estimation and other complex air-sea exchange assessments. An integrated modelling system consisting of WRF and storm surge models is extensively utilized to investigate TCs. For example, Lee *et al*.[15] utilized the four-dimensional nudging technique (FDDA) in the WRF-ARW model coupled with the ROMS ocean model to simulate the intensity and pressure fields of Typhoon Morakot. The integrated simulation generated surge estimates that closely aligned with observations. Lakshmi *et al*.[12] also reported skilful storm surge estimations with the integrated modelling of WRF and a hydrodynamic model, resulting in accurate simulations of TC Hudhud and Phailin. TCs undergo several changes in the track and intensity from the period of cyclogenesis till the weakening, which in some instances is a challenge to capture by regional models like WRF. Capturing the changes in the track and intensity of tropical cyclones from their formation to decay can be challenging for regional models such as WRF. The accuracy of weather predictions, particularly for complex and intense weather events, can be impacted by limitations of the WRF model and data assimilation techniques. These limitations include sensitivity to initial and boundary conditions, uncertainties in physical process parameterization, and challenges in assimilating non-conventional data sources. Ensuring appropriate assimilation techniques and quality control of observational data are crucial to address these limitations.

For dynamic downscaling of the meteorological variables (simulated by the global models) high, resolution regional climate models (RCMs) like WRF is extensively used[16]. RCMs can deviate from actual meteorological fields over time or during model simulations, resulting in discrepancies with actual observations and high bias in the simulated results. To address this issue, bias correction techniques are necessary. Inaccurate predictions of tropical cyclones can have severe consequences for disaster management and mitigation efforts in hazard-prone areas, including loss of life, property damage, false alarms, economic losses, and hindering relief efforts. It is crucial to improve the accuracy of tropical cyclone predictions through bias correction and modern data assimilation techniques to enhance disaster management and mitigation efforts and ensure the safety and well-being of people in hazard-prone areas. Bias correction can be implemented in RCMs using corrective terms or modern data assimilation techniques. The data assimilation technique depends on the availability of reliable observation data, which is a challenge during extreme weather events. The nudging technique applies an additional corrective term to the prognostic equations based on the difference between the model state and the observational reference field[17]. This method can be applied at all the model levels, but nudging at the planetary boundary layer (PBL) is not advisable[18]. Several previous studies have applied it in the WRF model[18–21]. Studies by Bowden *et al*.[20], Otte *et al*.[19], Liu *et al*.[16], Omrani *et al*.[21], & Bullock *et al*.[22] reported significant improvements in simulated variables when compared with observations in the WRF model when nudging was incorporated

Considering all the above discussions, this study has been undertaken to analyse the GPU-based WRF-ARW model performance (https://wrfg.net/wrfg-download/) in simulating the track and intensity of this unique cyclone. Most operational models could not pick up Vayu's unique steering, leading to high track error[1]. This study also aims at understanding the related synoptic features of the cyclone by comparison with satellite estimates and reanalysis datasets. The simulated parameters like wind speed, sea level pressure, and other critical synoptic features of the cyclone are compared with the satellite observations from the ASCAT scatterometer and

reanalysis dataset ERA-5. TCs undergo complex interactions during their lifecycle, influenced by the warm ocean temperatures[23–25]. SST has been proven to directly influence the intensification of TCs[26]. A similar conclusion is reported in several other works[27–29]. Thus, understanding the simulated air-sea interactions through the SST changes is also pertinent to understanding the model's reliability. Therefore, the present study also attempts to understand the reliability of the WRF-ARW model with a chosen set of physical settings in simulating the synoptic features of a unique TC Vayu. The study is planned to test the model's response with two different initial conditions (IC), GFS data and NCEP-FNL data, with and without external SST input. Finally, the best possible IC combination is simulated using a four-dimensional data assimilation nudging technique. Since caution should be taken while using the nudging parameters in the PBL layer[16], variables within the PBL layer were not nudged. The objective of the study is to understand some of the essential aspects of the rare TC Vayu as given below:

1. Simulation of GPU-WRF with and without external SST input with GFS and NCEP-FNL initial conditions, further apply analysis nudging method and estimation of the deviations of the simulated tracks from the one observed by IMD.
2. Comparison of simulated synoptic characteristics of the TC, such as wind speed, sea level pressure, low-level relative vorticity, relative humidity profile, wind speed profile, temperature anomaly, thermal instability, vertical wind speed shear with available IMD observations, satellite estimates, and reanalysis dataset.

2 Model Description, Methodology, Experimental Setup, and Datasets Used For Comparison

2.1 Model Configuration and Experimental Setup

The non-hydrostatic version of the WRF-ARW[30] model is used to understand cyclone Vayu's track intensity and synoptic features. This study opted for the GPU-based version of the WRF model over the conventional CPU-based version owing to faster computation. Increased efficacy of the WRF model with GPU cores is demonstrated in previous studies by Mielikainen *et al.*[31,32]; Huang *et al.*[33].

The GPU-based WRF (https://wrfg.net/wrfg-download/) is initiated with two different initial meteorological boundary conditions, NCEP-FNL data available at six hourly intervals at 1° spatial resolution from https://rda.ucar.edu/datasets/ds083.2/and GFS data from http://rda.ucar.edu/datasets/ds084.1/ available at six hourly intervals at 0.25°× 0.25° spatial resolution. Four experiments are conducted with and without time-varying sea surface temperatures (SST) input obtained from the real-time global SST database from the National Centers for Environmental Prediction[34], available daily at a spatial resolution of 0.083° × 0.083° (both in Latitude and Longitude), with a 9 km single model domain (Fig. 1) with 51 vertical pressure levels. The simulations are initiated from 8 June, 00 UTC 2019, till June 17, 21 UTC to fairly cover the storm's lifecycle with an initial 48-hour spin-up. Four simulations were conducted with GFS and NCEP initial conditions, with and without SST input. Initial track comparisons with IMD best track showed that simulations with GFS data and SST input gave relatively lower track error, but the distinct leftward bias was seen in the simulated tracks. Thus a four-dimensional data assimilation nudging (fdda) was applied to the GFS simulations with SST input from NCEP SST data (referred to as WRF_GFS_SST_nud). The physical parameterization schemes are kept similar in all the simulations given in Table 1. The model is simulated at three-hourly intervals with topography data of 10m spatial resolution from the US Geological survey

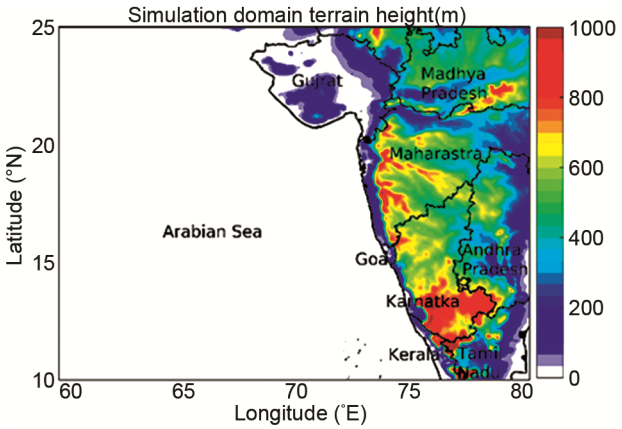

Fig. 1 — WRF simulation domain showing the terrain height (m).

Table 1 — Model parameterization schemes

Atmospheric process	Scheme used
Cloud microphysics	WSM 6 scheme
Longwave radiation	Rapid Radiative Transfer Model
Shortwave radiation	Rapid Radiative Transfer Model
Surface layer	Thermal Diffusion scheme
Land surface model	Noah Land Surface Model
Planetary boundary layer	Yonsei University scheme
Cumulus parameterization	Kain–Fritsch Scheme

topography in all the experiments. The physical settings of the model are adapted from the previous successful compilation of the model for TC-related studies for the Northern Indian Ocean. Several physical settings are available for the model in terms of the choice of convection, cumulus, land surface, etc. However, no unique parameterization scheme can successfully represent a tropical cyclone's dynamic features[12]. Thus, considering the vast variety of parameterizations available, several performance evaluations of the WRF-ARW model for a tropical cyclone, several previous studies have focused on TC-related research, particularly in the Northern Indian Ocean (NIO)[7–9,11,35,36]. Choice of cumulus convection, surface heat, moisture, momentum fluxes, and vertical mixing in the Planetary Boundary Layer, PBL determine the cyclogenesis and rapid intensification of tropical cyclones[37], which is regarded as a significant hurdle for numerical weather prediction models[38]. The PBL and convection schemes are essential factors in TC generation, as the momentum flow in PBL is important. The PBL scheme of the present study is chosen based on Osuri *et al.*[7]. Results of the study indicated that the YSU PBL scheme and KF convection scheme of the model lead to skillful capture of the track, intensity, and rainfall distribution of the TCs of the Northern Indian Ocean. The 9 km grid resolution of the study is chosen based on Osuri *et al.*[11]; the study showcased a successful simulation of 100 TCs during 2017-2011 with three grid resolutions 27, 18, and 9km. The results indicated a significant improvement in track and intensity predictions by the 9 km resolution simulations. A 9 km single-domain simulation of the model successfully compiled a cyclonic case study of the Northern Indian Ocean three days in advance by Nadimpalli *et al.*[6]. A single domain is computationally less intensive, making it an optimal choice for the study considering the computational limitations with a~8GBGPU used in the present study. Cumulus parameterization and other physical settings like the land surface model and radiation schemes for this study are adapted from Several previous similar application of WRF for Northern Indian Ocean TCs[6–9,11,36]. All these studies showed the model's credibility with the selected set of parameterizations for TC-related studies for the Northern Indian Ocean.

2.2 Reanalysis Datasets Used

The synoptic parameters of TC Vayu are compared with that of the well-known reanalysis dataset ERA-5. Simulated wind speed (m/s), relative humidity (%), temperature anomaly (K), thermal instability (K), and vertical wind speed shear (m/s) are compared with that of the ERA-5 dataset. ERA-5 stands for ECMWF fifth generation reanalysis dataset. This new reanalysis dataset will replace its predecessor, ERA-interim reanalysis. The ERA-5 model is based on the Cy41r2 integrated forecasting system (IFS), which was operational in 2016; thus, the dataset has the benefits of several years of bias correction, data assimilation, improved core dynamics, and new model physics developments. Using physical laws, reanalysis combines model data with observations from around the world to create a globally complete and consistent dataset. This principle, known as data assimilation, is based on the method used by numerical weather prediction centers, in which a previous forecast is combined with newly available observations in an optimal way every so many hour (12 hours at ECMWF) to produce a new best estimate of the state of the atmosphere, known as analysis, from which an updated, improved forecast is issued. Reanalysis works similarly but at a lower resolution to provide a dataset spanning several decades. Because reanalysis is not constrained by the need to issue timely forecasts, there is more time to collect observations and, when going further back in time, to allow for the ingestion of improved versions of the original observations, all of which benefit the quality of the reanalysis product. The dataset is available freely from https://cds.climate.copernicus.eu/cdsapp at several pressure levels and surfaces with a spatial resolution of 31 km at hourly intervals and an uncertainty estimate from an ensemble[39].

2.3 Scatterometer Data Used

Daily average ASCAT (a C band scanning) scatterometer winds (10m) available at 25 km spatial resolution is used for comparison with the simulated surface winds during the cyclonic period from 10 June to 17 June 2019. Daily average gridded winds are freely available from http://apdrc.soest.hawaii.edu/las/v6. ASCAT takes five days to cover the globe (with two 550 km wide swaths) and can capture wind speed, WSs ranging from 4 to 24 m/s. It has an accuracy of 1.2 m/s for WS and 18 for WD, respectively[40]; details of the product can be obtained from Figa & Stoffelen[41]. ASCAT wind products have previously been validated and are comparable with observations[42,43].

3 Results and Discussions

3.1 Comparison of Simulated Tracks with the Best Track Estimates from IMD (Indian Meteorological Department)

As illustrated in Fig. 2, the simulated tracks of cyclone Vayu from 00 UTC 10 June to 17 June with different ICs are compared with the best track information from IMD. Fig. 2 shows that including external SST (Sea Surface Temperature) reduces track error. Considering the model simulated with the GFS_SST dataset shows the least mean track error (Table 2), an additional set of simulations is conducted where the model is initiated with GFS data. External SST input and analysis nudging technique is applied to the model in wind temperature and mixing ratio field throughout the simulation period, referred to as WRF_GFS_SST_nud hereafter. It is evident from the figure that analysis nudging improves track estimates, thereby reducing track error (Fig. 3). An increase in track error (~ 50 km) is seen in WRF_GFS_SST_nud at 00 UTC 16 June (Fig. 3(a)). This might be attributed to the incorrect representation of the air-sea interactions over the region during the cyclone activity in the global model GFS due to a lack of sufficient in-situ observations over the Arabian Sea[1].The model's inability to capture the storm's steering on 16 June is also reported by Singh *et al.*[44]. This disparity is seen in all the simulations (Fig. 2), indicating the issues of all the well-known datasets to capture the complex dynamics leading to this unique recurving of the cyclone. As per the initial satellite imagery from INSAT at 06 UTC on 13 June, the system was found close to the Gujarat coastline. Based on the operational NWPs, IMD predicted the landfall of Vayu on the Gujarat coastline on 15 UTC 12 June, leading to the emergency public evacuation. However, the system was under the influence of mid-latitude westerlies, which led the system to skirt the Gujarat coastline, moving further north-eastwards resulting in a very high landfall error from IMD. However, the results of the present study indicate that the inclusion of the nudging method resulted in improved track (Fig 2(b) & Fig. 3(a) and intensity estimates (Fig. 3(b & (c)). Thus, further analysis of the cyclone dynamics is done on the

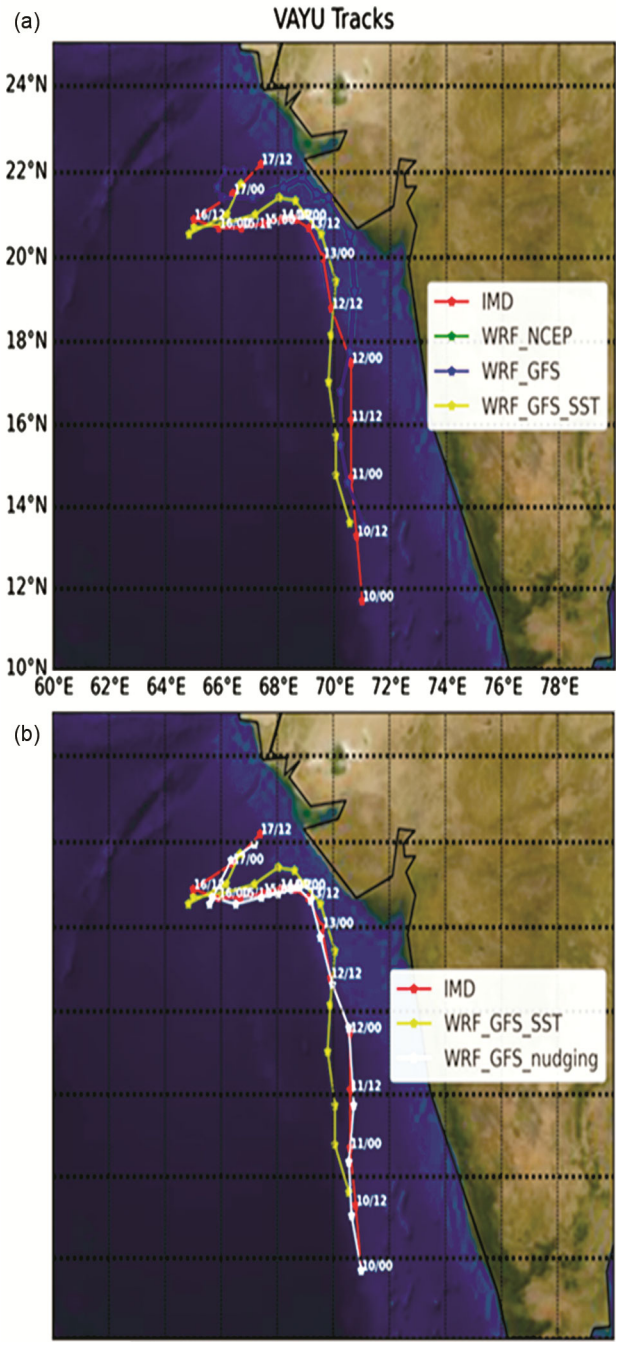

Fig. 2 — (a) Comparison of WRF simulated tracks, without nudging technique (b): Comparison WRF simulations with GFS data, SST update, and nudging technique with best track estimates from IMD.

Table 2 — Mean error (ME), Standard Deviation (SD) of the simulated track, intensity of cyclone Vayu against that of IMD

Dataset	Track error(km)		Max wind speed(m/s)		Min Sea level Pressure(hPa)	
	ME	SD	ME	SD	ME	SD
NCEP_SST	94.1	101	5.5	7.09	25.4	7.01
GFS_SST	82.42	92.13	5.17	6.66	24.91	6.68
GFS	106	72.15	5.76	7.34	15.13	10.82

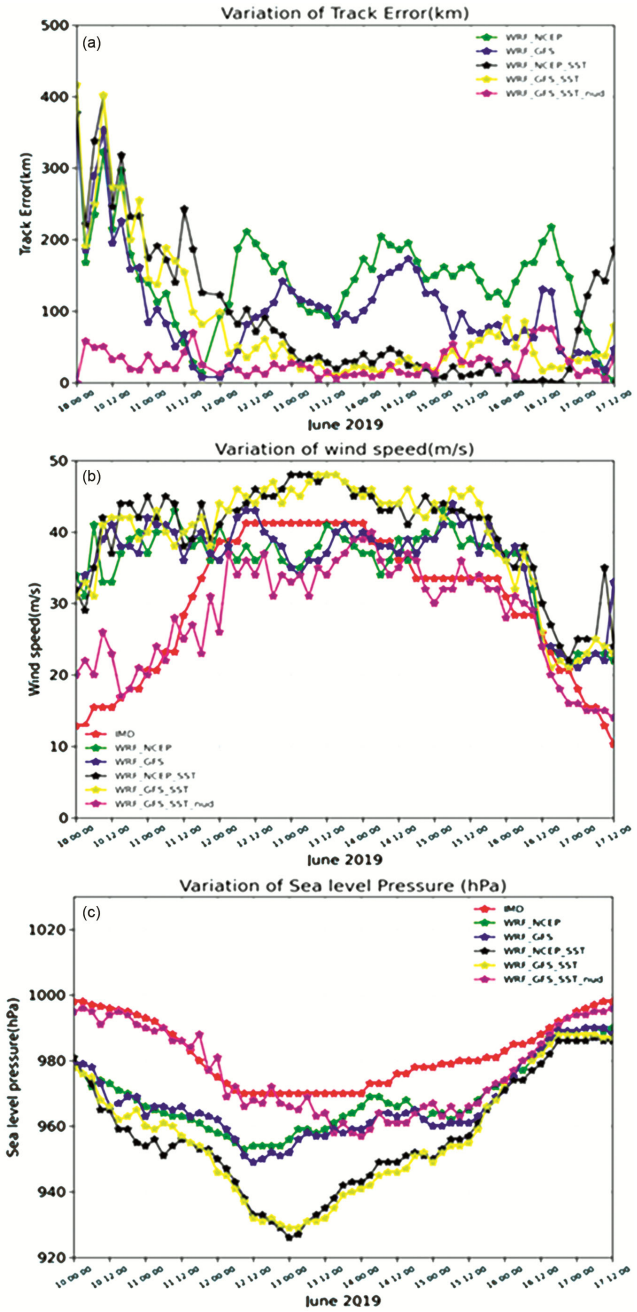

Fig. 3 — (a) Variation of track error (km), (b) maximum surface wind speed (m/s), and (c) minimum sea-level pressure (hPa) during the cyclone period.

WRF_GFS_SST_nud. Several interactions of the wind fields of Vayu with that of mid-latitude westerlies led to the unique track of the cyclone with two distinct steerings, which was proven to be a challenge for the operational forecasting models initially predicted a landfall over the Gujrat coastline[1]. The results indicate that using analysis nudging can improve track estimates and skillful capture of such a unique storm track. WRF_GFS_SST_nud showed a skillful capture of the initial vortex of the storm with very low track error (Fig. 2(b)), indicating incorporation of NCEP SST leads to improved track estimates, which in agreement with a similar application of influence of different SSTs into WRF_ARW model for TC Vayu by Singh *et al.*[44]. The successful capture of the system's north-westward steering with the model's current physical settings indicates the reliability of the model setup, which was reported to be a challenge by Singh *et al.*[44] even with similar SST input but without analysis nudging. The mean intensity error of 1.64 m/s and 5.39 hPa (Table 2) with the 48-hour spin-up of the model indicated an improved performance compared to a similar study of the VSCS. The results show the positive impact of the nudging technique along with the selected set of the parameterization scheme.

3.2 Comparison of Simulated Wind Speed with ERA-5 and ASCAT at Various Stages of Cyclone Vayu

An accurate estimation of surface wind speed is essential to mitigating the impending loss caused by TCs. Fig. 4 (a&b) illustrates the spatial distribution of the model's daily mean 10 m wind speed (top panel) and ERA-5(bottom panel), and ASCAT scatterometer (bottom panel). The simulated winds and ERA-5 data are gridded to the ASCAT spatial resolution of 25 km before comparison. The recurvature of the cyclone track moving away from the Gujrat coastline on 13 June is seen in all the datasets, but as evident from the figures and Table 3, the model simulates a stronger storm in terms of surface wind speed compared to ERA-5 and ASCAT. As the system underwent rapid intensification from cyclonic to the super cyclonic stage on June 11, 12 UTC, the intensification of surface wind speed is seen in the spatial distribution of daily average wind speed in Fig. 4. At the SCS stage of the storm, the estimated daily mean wind speed of the model is 27.03 m/s, but that of ERA-5 is 19.48 m/s, and that of ASCAT is 23.11 m/s. According to IMD RSMC reports[45] & Mishra *et al.*[1], the system further intensified into a VSCS category from June 11, 18 UTC onwards. The simulated daily average surface wind speed is estimated to be maximum on 14 June at 33.25 m/s, but that of ERA-5 is 22.5 m/s. The model skillfully captures the reduction of wind speed intensity; at this stage, the model is again seen overestimating the wind speed compared to the ERA-5 dataset. ASCAT surface winds match the simulated winds more closely than

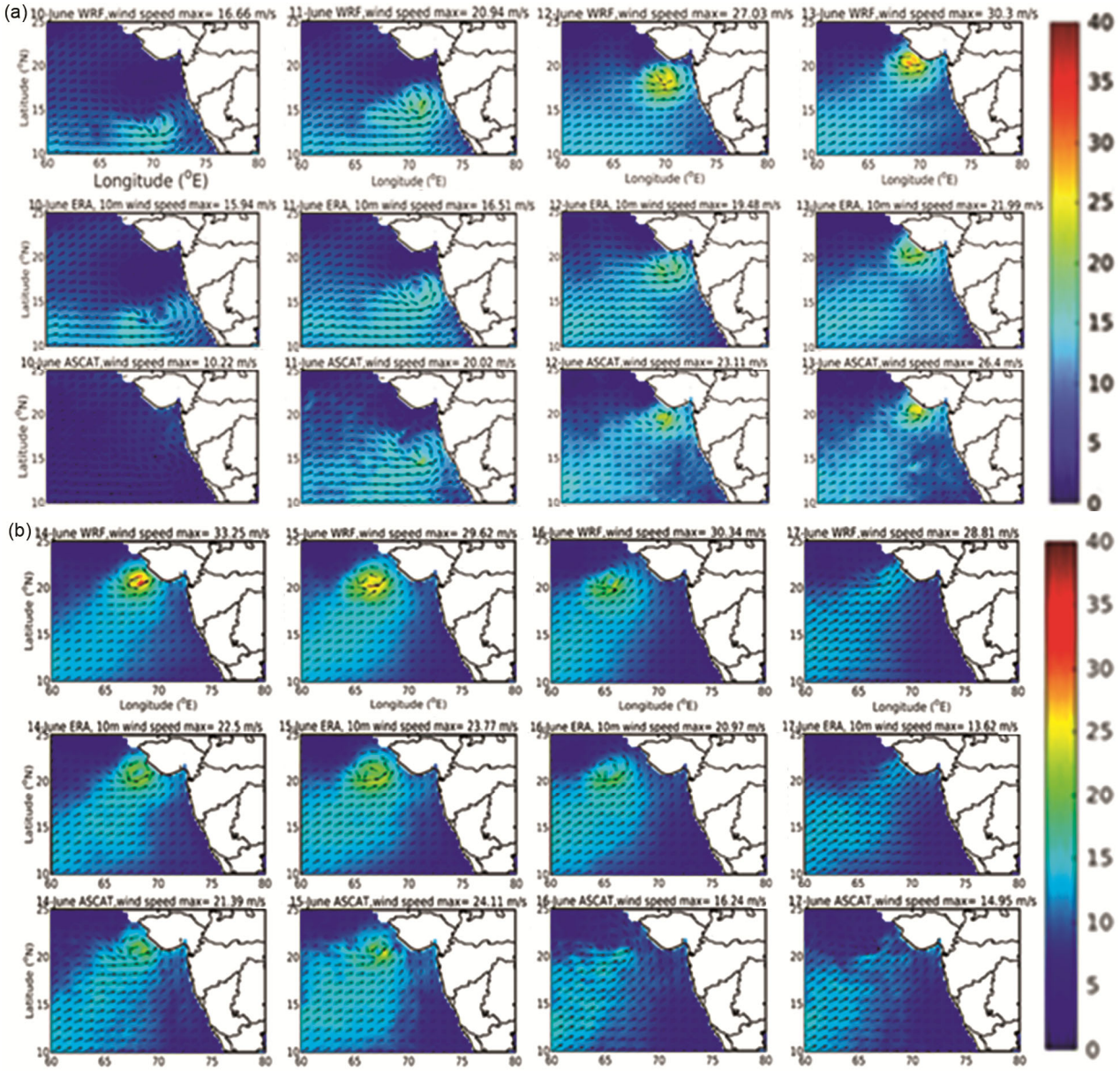

Fig. 4 — Spatial distribution of daily average 10 m surface winds of WRF (top panel) and that of ERA-5 (bottom panel) and ASCAT (bottom panel), (a) for 10th to 13th June 2019, (b) for 14th to 16th June 2019.

Table 3 — Comparison of daily average maximum surface wind speed (m/s)

June 2019	WRF_GFS_SST_nud (m/s)	ERA-5(m/s)	ASCAT(m/s)
10	16.66	15.94	10.22
11	20.94	16.51	20.02
12	27.03	19.48	23.11
13	30.3	21.99	26.4
14	33.25	22.5	21.39
15	29.62	23.77	24.11
16	30.34	20.97	16.24
17	28.81	13.62	14.95

the reanalysis dataset. Tropical cyclones undergo rapid intensification where the maximum wind speed increases over 15 m/s within 24 hours[46], which is still a significant hurdle in numerical forecasting[38]. Forecasting RI in cyclones is still a significant challenge as there is still a poor understanding of the factor leading to RI[47]. Thus to understand the model's capability to capture the rapid intensification of the system vertical profile of wind intensity through the eye of the cyclone is analyzed. Fig. 5 depicts the vertical cross-section of the wind speed profile

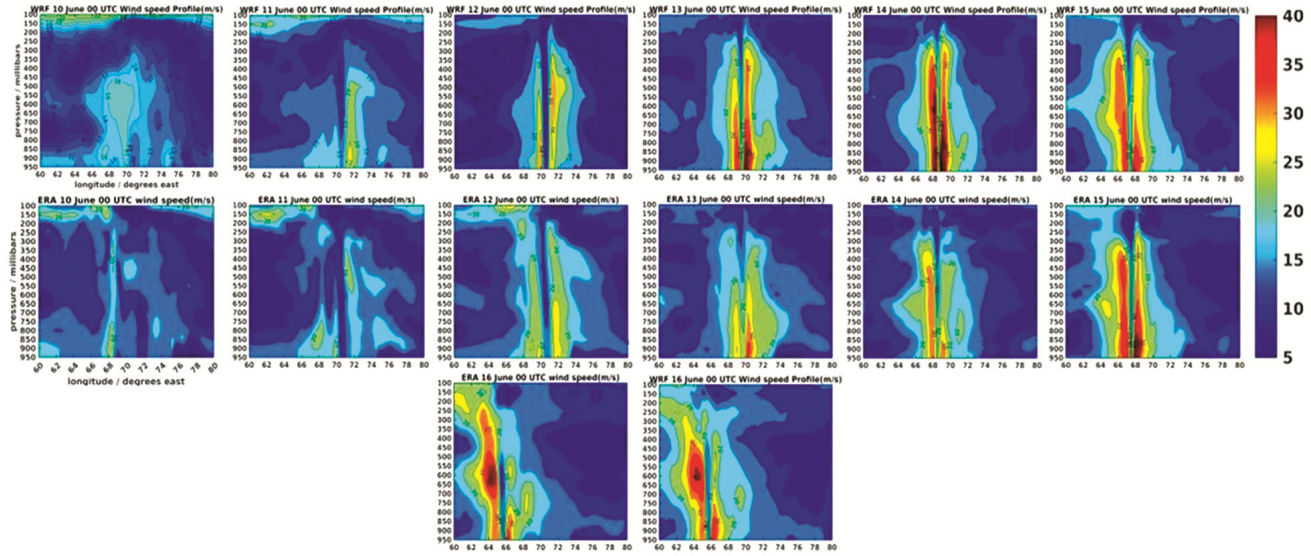

Fig. 5 — Vertical cross-section of wind speed through the eye of the cyclone for WRF and ERA-5 valid through 00 UTC of each day from 10 June to16th June 2019.

through the eye of the storm at 00 UTC each day from 10 June to 16 June 2019. The formation of a well-delineated eyewall with increased wind speed from the outer to the inner wall is evident in both datasets. On 12 June, the system maintained a matured VSCS stage; the inner wall wind speed is estimated to be 30 m/s, increasing to >40m/s from 13 June onwards. The weakening of the system on 16 June to the cyclonic stage is well captured by the model and ERA-5, where the vertical structure is similar. However, the model again is overestimating compared to ERA-5. The study results agree with the previous study by Hodges *et al.*[48], where a similar underestimation of cyclonic wind intensity by reanalysis datasets is reported. A weaker eyewall formation by ERA-5 datasets during a TC is also reported by Subrahamanyam *et al.*[49]. Tropical cyclones are dynamic phenomena accompanied by heavy rainfall, which leads to attenuation of wind speed intensity in scatterometer estimates[50] which might have attributed to the underestimation of wind intensity in ASCAT. Overall, the results indicate a skillful capture of the rapid intensification of the intensity by WRF with the present set of parameterization schemes.

3.3 Comparison of the Vertical Cross-Section of relative Humidity (%) and Temperature Anomaly (k) Through the Eye of the Cyclone of WRF and ERA-5

Higher relative humidity (%) is associated with the rapid intensification of tropical cyclones[51]. Fig. 6 (a&b) depicts the variation of the vertical profile of RH (%) at 00 UTC of each day from 10 June to 16 June through the eye of the cyclone. It is evident from the figure that the initiation stage of the cyclone on 10 June at 00 UTC shows a high relative humidity profile in the mid-troposphere (500-700 hPa) which favors rapid intensification. The storm underwent rapid intensification on the morning 00 UTC of June 12, 12 hours prior to the RI on 11 June at 12 UTC; the model shows a high RH% of ~100 %, indicating the moisture present in the storm center is higher than the RH% 12 hours prior to the onset of RI, conditions favoring RI onset within 24 hours[47]. As the system maintained the matured VSCS (Very Severe Cyclone Storm) stage from June 11, 18 UTC onwards, an exceedingly high RH (%) extending to 300 hPa was seen from 12 June to 15 June. The reduction in intensity to the cyclonic stage started from 16 June onwards when the system weakened to CS (Cyclonic Stage). A similar reduction in intensity is reflected in both data sets decrease in RH (%) on 16 June. The results indicate that the model with the current set of physical parameterizations can capture the rapid intensification of the system as seen by the high RH (%) >90% throughout the various stages of the cyclone. The anomalously high moisture content from the initiation stage made favorable conditions for an accurate onset of RI. The weakening stage of the cyclone model and ERA-5 show similar dissipation of the high RH (%) profile. Temperature anomaly is related to the formation of the storm's warm core, as the release of latent heat is one of the essential contributors to the

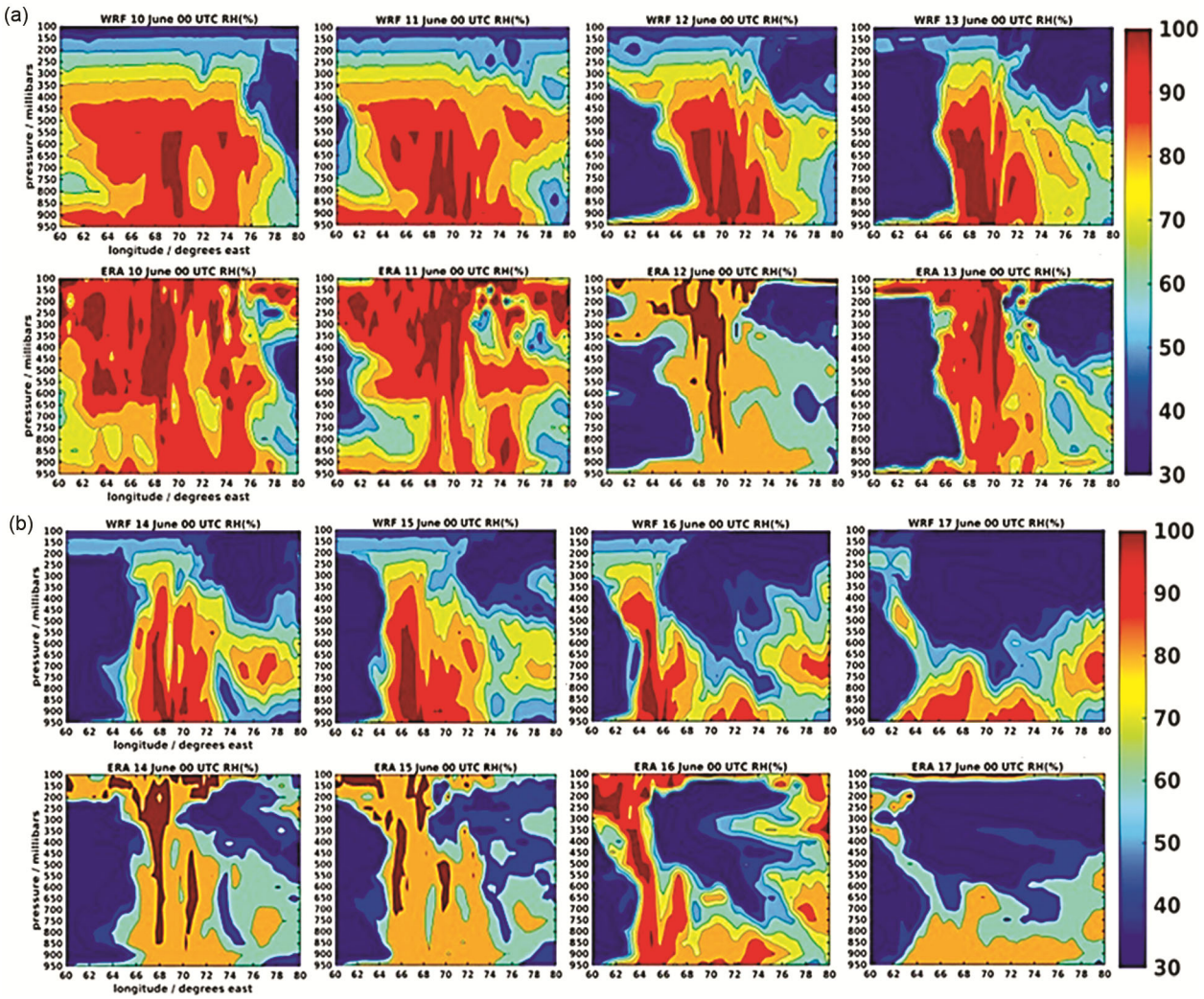

Fig. 6 — Variation of RH (%) through the eye of the cyclone for WRF (top panel) and ERA-5 (bottom panel) valid for (a) 00 UTC of 10-13 June 2019, (b) 00 UTC of 14-16 June 2019.

formation of the warm core. The vertical extension of the cyclone's warm core indicates the storm's thermal profile[52]. Fig. 7(a&b) shows the vertical profile of temperature anomaly (k) of the model (top panel) and ERA-5 (bottom panel) through the eye of the cyclone from 00 UTC 11 June to 00 UTC 16 June 2019.As the storm underwent rapid intensification on 12 June, the temperature anomaly is estimated to be about 4 k when the warm core is seen extending to 200 hPa. WRF and ERA-5 show a temperature anomaly of 4-6 k extending to the upper troposphere at the mature stages of the storm.

3.4 Comparison of Simulated Thermal Instability of WRF and ERA-5 at Various Stages of Cyclone Vayu

The developmental phase of a TC is related to intense convective activity, which is again related to mid-tropospheric instability. The difference in temperature between 500 hPa and 850 hPa is considered to measure the mid-tropospheric instability Kotal *et al*.[53]. Lower values of this thermal instability indicate the presence of a warm core. A decrease in thermal instability suggests an increase in storm intensity as the temperature in the mid-troposphere increases with intensification due to latent heat release Ganesh *et al*.[54]. (Fig. 8(a&b)) shows the variation of mid-tropospheric instability for the model and ERA-5 at 00 UTC each day from 10 June to 17 June 2021. At the developmental phase of the cyclone, the tropical disturbance is characterized by the middle troposphere instability related to the temperature difference between 850 hPa and 500 hPa, which is related to intense convection and warming of the core.

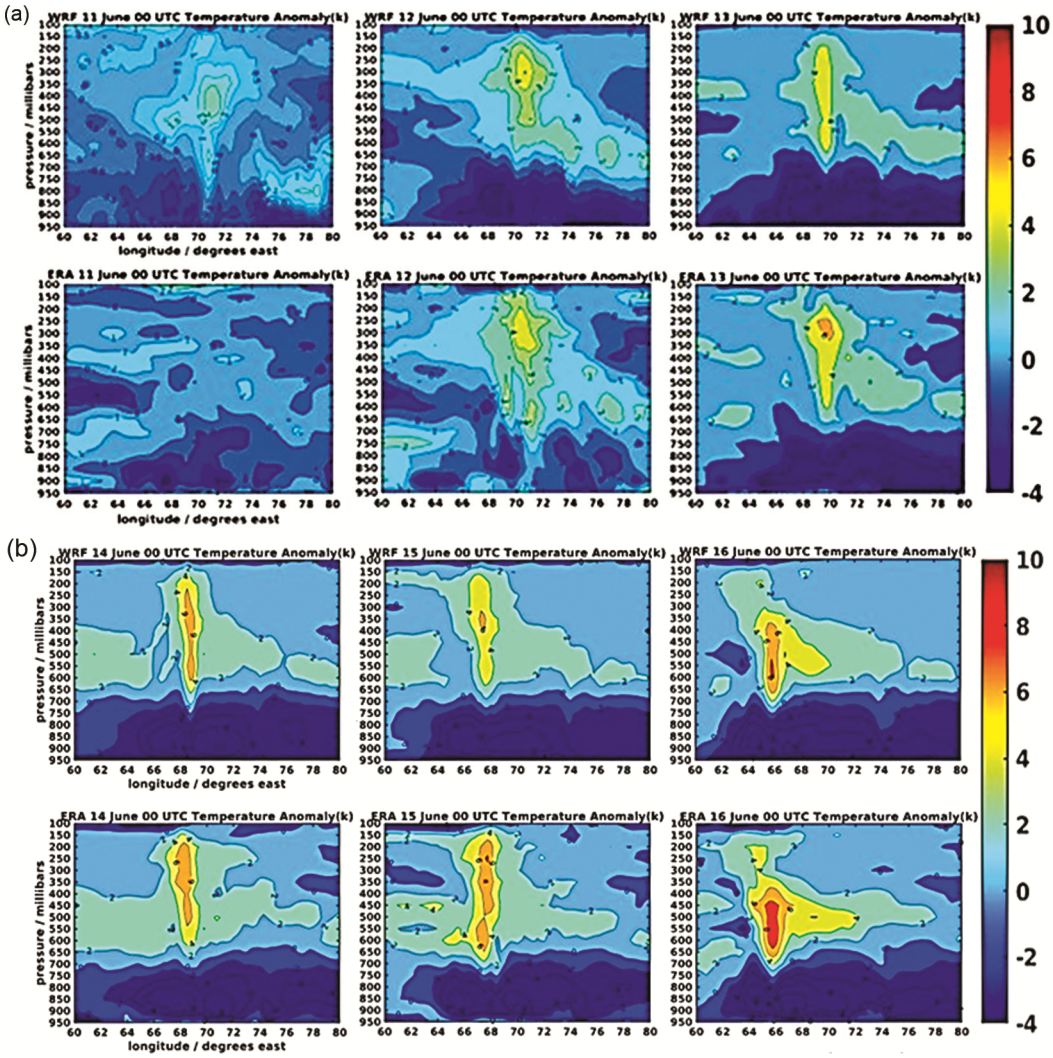

Fig. 7 — Temperature anomaly (K) of the storm through the eye for WRF (top panel) and ERA-5 (bottom panel) for (a) 00 UTC of 11-13 June 2019, (b) for 00 UTC of 14-16 June 2019.

3.5 Comparison of the Spatial Distribution of Vertical Wind Speed Shear (m/s) of WRF and ERA-5 at Various Stages of Cyclone Vayu

To understand the model's credibility in simulating the vertical wind speed shear (VWS) during various stages of cyclone Vayu, the vertical wind speed shear (m/s) at 200-850 hPa is shown in Fig. 9 (a&b) for WRF (top panel) and ERA-5 dataset (bottom panel) for 00 UTC 10 June to 00 UTC 17 June 2019.Higher values of VWS around the storm center are known to negatively impact the system's intensification. According to Linda *et al.*[55], a critical value of wind shear of approximately 10 m/s indicates the dissipation stage of the storm and values lower than 10 m/s favor intensification. At the initial stages of the cyclone development, the circulation may not extend till 200 hPa; thus, vertical wind speed shear is not pertinent[47] at the early depression stage on 10 June 2019, which is seen organizing itself as the storm undergoes intensification. The spatial distribution of VWS in Fig. 9 shows that the locations of lower WVS are collocated with the center of the storm. As the cyclone weakened on 17 June at 00 UTC (Fig. 9), an increase of WVS of approximately 20 m/s was seen, leading to further storm dissipation.

3.6 Comparison of the Spatial Distribution of Low-level Relative Vorticity (RV) of WRF and ERA-5 at Various Stages of Cyclone Vayu

According to Gray (1968), the low level (850 hPa) relative vorticity of a cyclone is one of the essential parameters of the dynamics of the cyclone and is a key factor affecting the intensity of tropical cyclones[56–58].The triad of shear, curvature, and

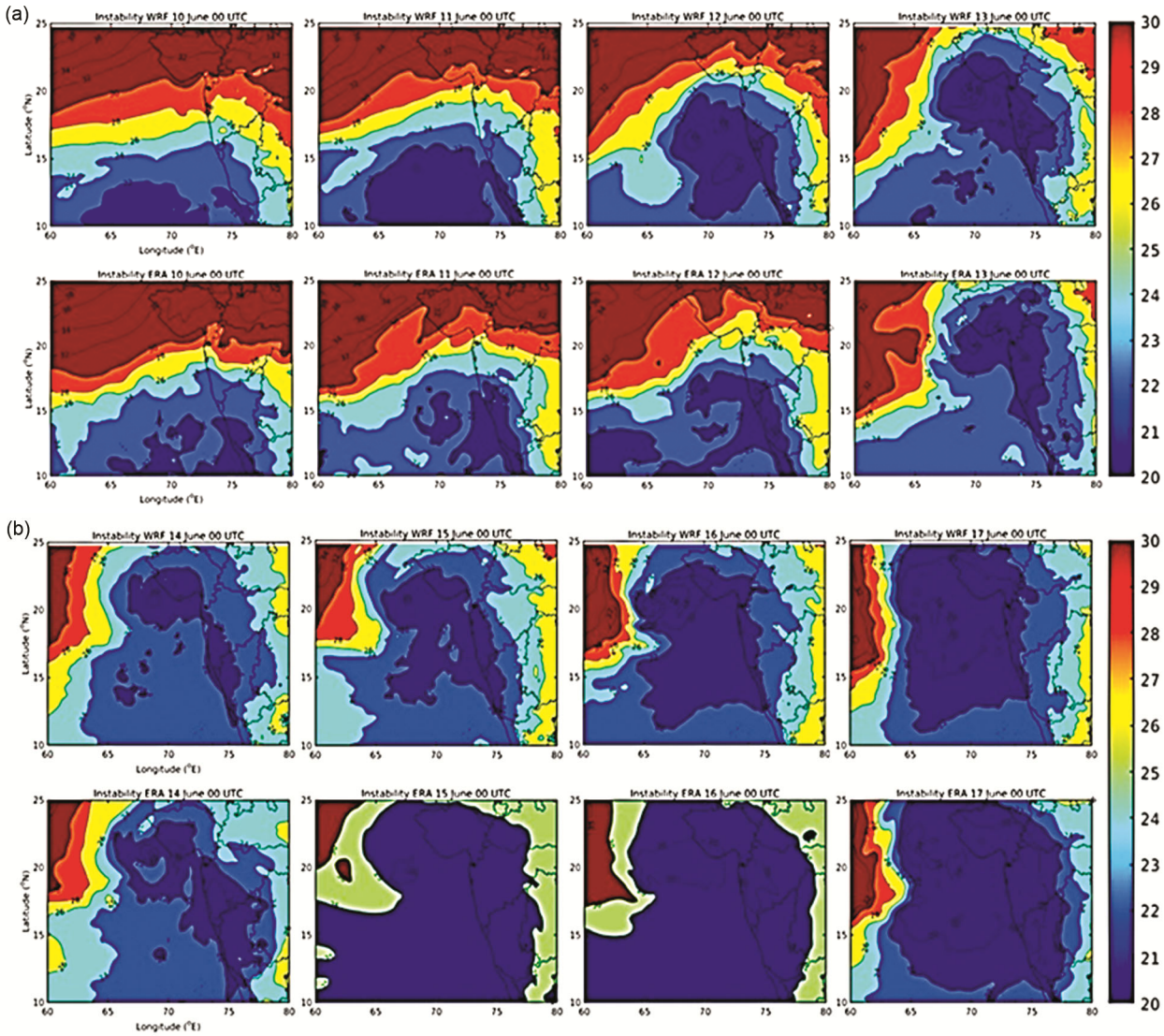

Fig. 8 — Variation of thermal instability at 00 UTC for WRF (top panel) and ERA-5 (bottom panel) (a) 00 UTC of 10-13 June 2019, (b) for 00 UTC of 14-17 June 2019.

Coriolis force contributes to the generation of vorticity in a cyclonic system. A positive and high value of RV in the lower troposphere is generally associated with favorable conditions for the formation and intensification of tropical cyclones, while a negative value is linked to the weakening of these systems. Fig. 10 (a&b) shows the spatial distribution of low-level relative vorticity at various stages of TC Vayu simulated by the model and the ERA-5 dataset. From Table 4, as discussed earlier, the model is seen as overestimating compared to ERA-5. At the matured VSCS stage of the cyclone on 12 June 00 UTC, the simulated storm has a strong low-level relative vorticity of approximately 171.20×10^{-5} s^{-1}, whereas ERA-5 is 86.10×10^{-5} s^{-1}. On 13 June 00 UTC, the center of high relative vorticity of the model and that of ERA-5 are not collocated, simulated storm center with high low-level vorticity of 221.49×10^{-5} s^{-1} is seen skirting away from the Gujrat coastline, but that of ERA-5 is seen closer to the Gujrat coastline with an estimated value of 139.59×10^{-5} s^{-1} which might be attributed to the erroneous estimation of storm dynamics in the reanalysis dataset owing to the scarcity of observation in the Arabian sea.

3.7 Genesis of VSCS Vayu and Madden Julian Oscillation (MJO)

Vayu originated from a low-pressure system on 9 June in the southeast and adjoining the east-central Arabian Sea. Previous studies have indicated that

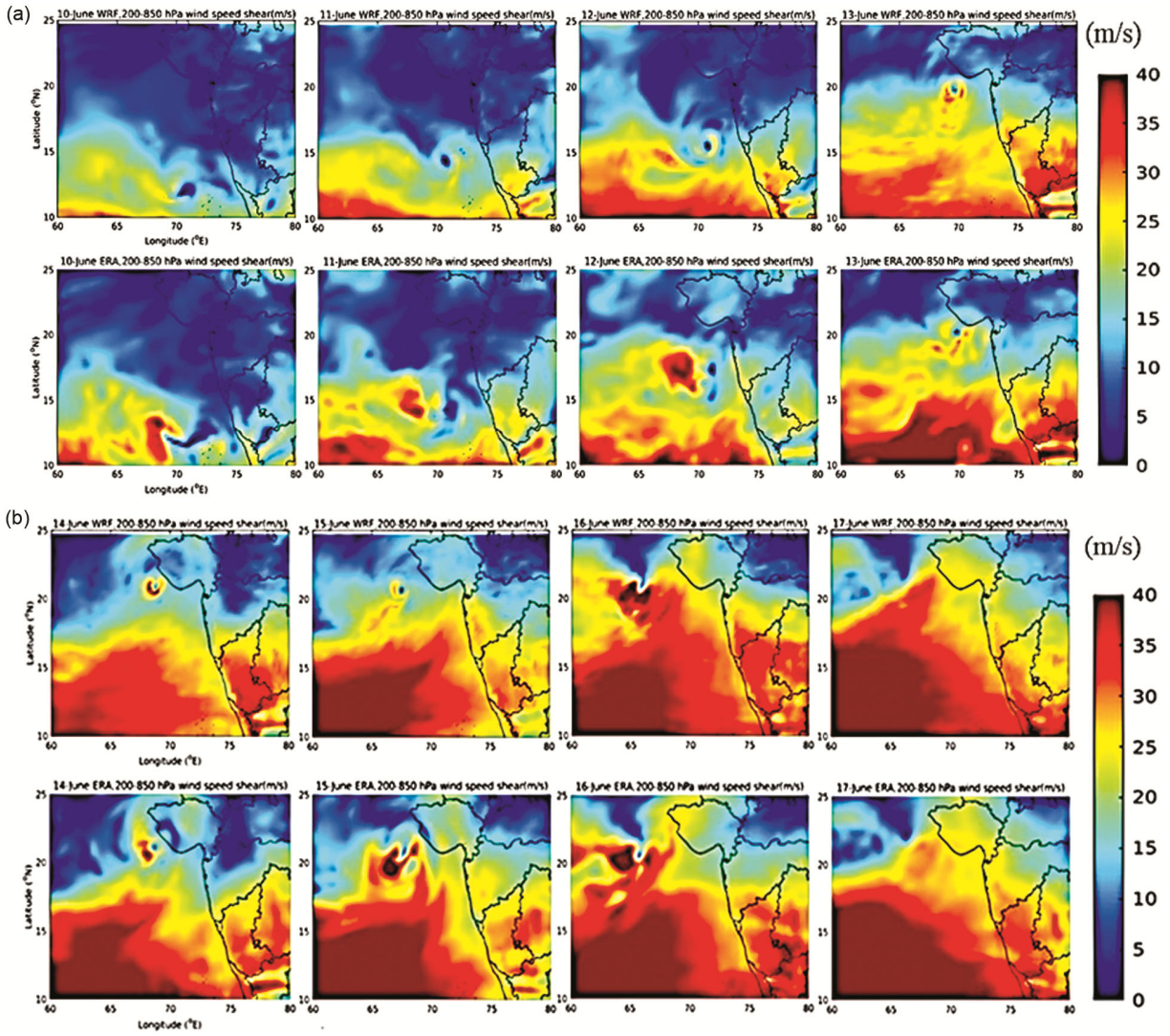

Fig. 9 — Spatial distribution of the vertical wind speed shear (m/s) over the simulation domain for the model (top panel) and ERA-5 (bottom panel) for (a) 00 UTC of each day from 10 June-13 June 2019, (b) 00 UTC of each day from 14 June-17 June 2019.

MJO, which is an eastward propagating band of a convective phenomenon in tropical regions, provides favorable atmospheric conditions for cyclone formation[59]. MJO (Fig. 11(b)) was in the second phase during the cyclogenesis, but later it was seen moving into phase 4 with an increase in MJO amplitude, favoring intense convection and cyclogenesis over the region. In order to understand the capability of the model to capture the genesis of cyclone Vayu, the tropical cyclone genesis parameter (GPP)[60,61] is estimated. Fig. 11(a) shows the spatial distribution of GPP from 00 UTC of 9 June to 12 June. Fig. 11 shows the gradual organization of the GPP zone at 00 UTC on 9 June with GPP>30, which is identified to be the threshold for cyclogenesis[60]. From 10 June onwards, clusters of GPP greater than the threshold are seen organizing themselves with spiral bands, subsequently moving along the observed cyclone track (Fig. 2), indicating a potential zone for cyclogenesis. On 11 June, 00 UTC, the GPP cluster affirmed the system maturing into a cyclonic storm, further intensifying into a matured VSCS on 12 June, 00 UTC. The results indicate the model's reliability in capturing the cyclogenesis from the depression stage in the southeast-central Arabian Sea, making the setup suitable for operational forecast studies.

3.8 Simulated Sea Surface Temperature (SST) with Sea Surface Height Anomaly (SSHA) During Various Stages of Cyclone Vayu

The influence of SST on the intensification of TCs is reinforced in several works of literature[27-29]. Warm waters provide favorable conditions for TC

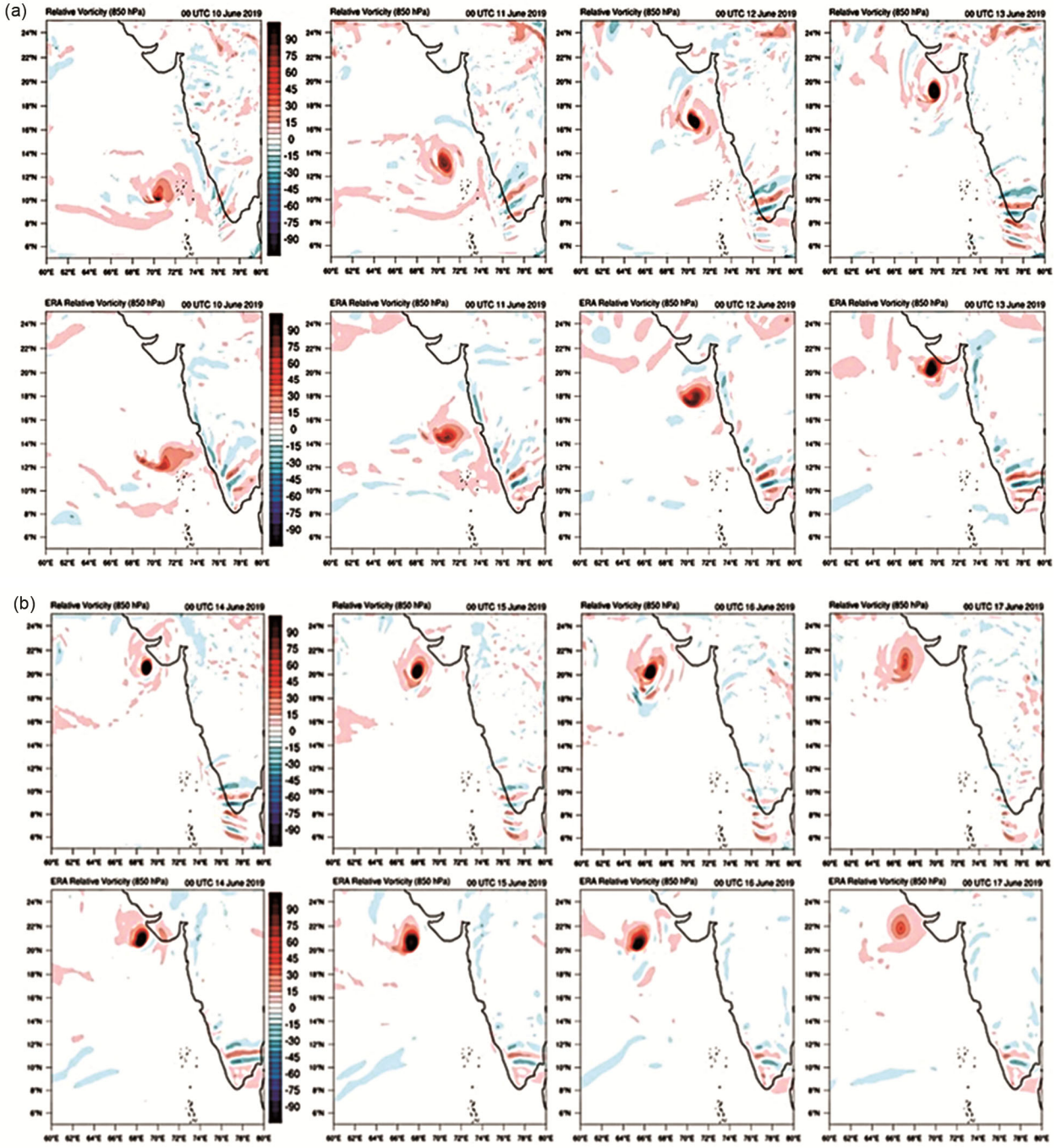

Fig. 10 — Spatial distribution of low-level relative vorticity (850hPa) for WRF (top panel) and ERA-5 (bottom panel) at 00 UTC of each day from 10 June to 17 June 2019.

intensification. The intensification of TCs is a complex phenomenon caused by intricate air-sea interactions[62]. Fig. 12 shows that the storm followed the gradient of high SST (> 30 °C), which was also conducive to rapid intensification. The system underwent rapid intensification from 11 June 12 UTC onwards, which is in agreement with the high SST, with all the processes favorable for the intensification. Previous studies over the Atlantic region showed that TCs moving over relatively high SST leads to rapid intensification[63,64]. After 16 June, there was a reduction in SST which led to an overall reduction in the heat fluxes causing the intensity to reduce and diminish as a depression. This overall process gave

negative feedback to the storm. The relationship between SSHA and the related hydrographic structure of the Northern Indian Ocean is depicted in past studies[62,65–67]. Fig. 12 shows the variation of simulated SST(C) with SSHA (cm) anomaly contours (obtained from European Copernicus Marine Monitoring Service) overlaid with IMD estimated the best track of the cyclone(colored dots). Several past studies have indicated the rapid reduction of SST along the track as the cyclone passes; this cooling leads to negative feedback to the TC, leading to a reduction in strength[68,69], Fig. 12 shows the cooling of the ocean surface as the storm passes. According to Mishra *et al.* [1]predicting the unique steering away from the Gujarat coast was initially a challenge for all the operational models; from 12 June 12 UTC, the unique recurving was captured. The present study shows the increased SST from 12 June (Fig. 12), which also contributes to such a unique track. The positive impact of the inclusion of external SST might be due to a change in enthalpy leading to changes in surface fluxes; this leads to negative feedback on the

Table 4 — Estimated values of low-level relative vorticity at various stages of cyclone Vayu

Date	Relative vorticity ($\times10^{-5}s^{-1}$) 850 hPa WRF	Relative vorticity ($\times10^{-5}s^{-1}$) 850 hPa ERA-5
10 June 00 UTC	86.86	47.74
11 June 00 UTC	76.69	70.57
12 June 00 UTC	171.20	86.10
13 June 00 UTC	221.49	138.59
14 June 00 UTC	359.93	175.39
15 June 00 UTC	213.23	180.31
16 June 00 UTC	186.75	141.06
17 June 00 UTC	61.49	41.23

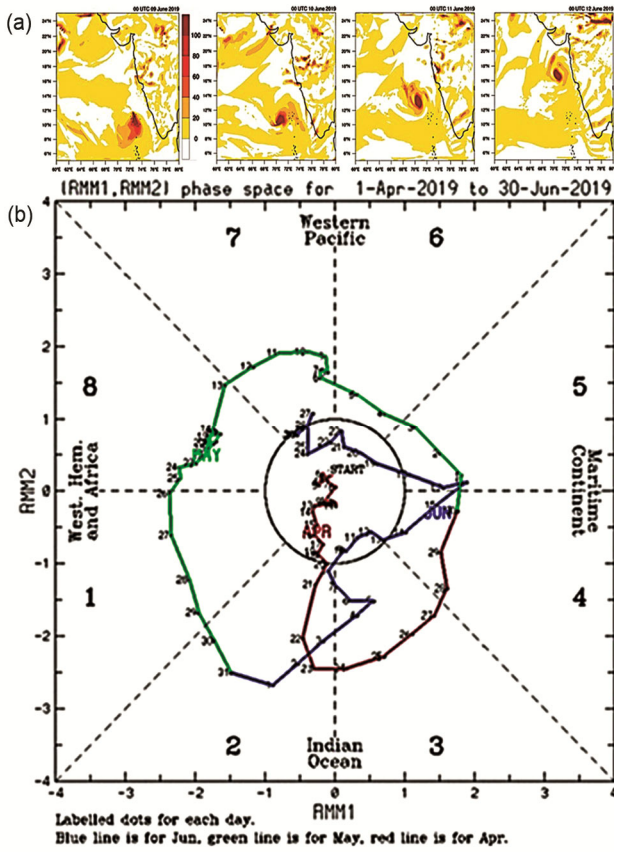

Fig. 11 — (a) Simulated Tropical cyclone genesis potential parameter (GPP) for 00 UTC of each day from 9 June to 12 June, (b) Phase diagram of Madden Julian Oscillation obtained from Australian Bureau of Meteorology April-May 2019. Colour denotes the progress of MJO in different phases when inside the black circle, denoted low amplitude and outside the circle indicates strong MJO with high RMM amplitude (Singh *et al*., 2020).

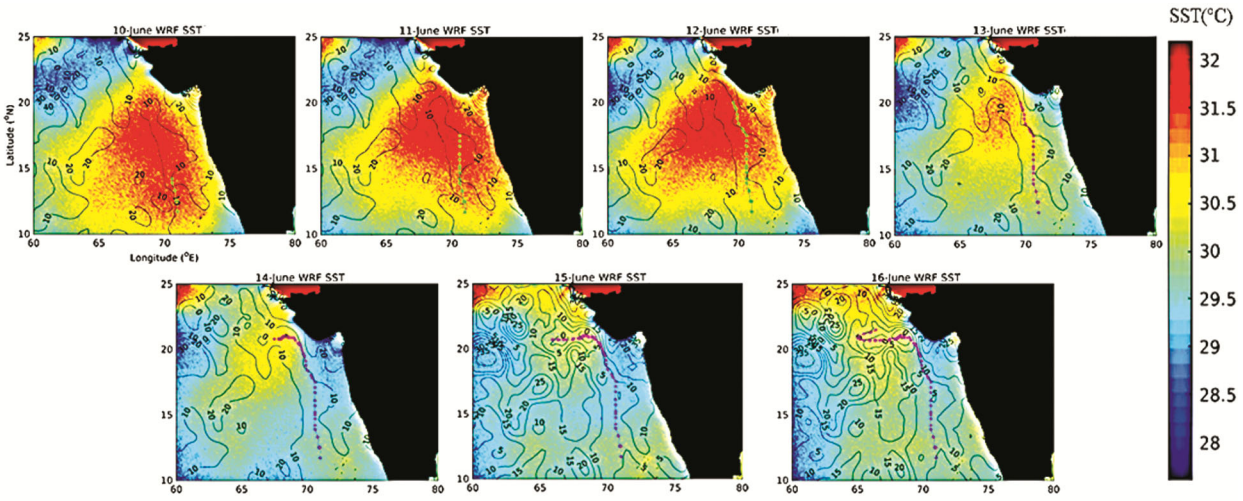

Fig. 12 — Variation of simulated SST with SSHA contours overlaid with the best track from IMD at various stages of cyclone Vayu.s

storm's strength through vertical mixing[44]. The formation of anticyclonic eddies represents the warm core. Higher SST coincides with the positive anomaly of ~10-20 cm, indicating higher regional heat content. Fig. 7-12 depicts the existing favorable thermodynamic conditions like high mid-troposphere RH (%) and the unstable atmosphere along with high SST (Fig. 12) are known to be conducive to the rapid intensification of the system[70].

3.8 Accumulated Cyclone Energy of Vayu

The accumulated cyclone energy (ACE) of a cyclone is a measure of the cyclone destruction potential proportional to the square of the maximum surface wind speed over the lifecycle of the cyclone. ACE is treated as a measure of the storm's kinetic energy[71]. The estimated ACE of the simulated cyclone Vayu is 9.35×10^4 $knts^2$, while that of the observed is 11.54×10^4 $knts^2$ over the lifecycle of the cyclone. The underestimation of ACE in the simulated cyclone is caused by the underestimation of maximum surface winds at the mature storm stage, as seen in Fig. 3. The estimated ACE of VSCS Vayu is approximately 0.51 times higher than the climatological mean of ACE of the Arabian Sea pre-monsoon cyclone, calculated based on the mean of 1990-2020[45].

4 Conclusions

VSCS Vayu originated from a low-pressure system in the Arabian Sea on 9 June 2019, which eventually matured into a very severe cyclone from June 11, 18 UTC onwards under favorable synoptic conations. The storm exhibited unique features in terms of track and intensity, as it recurved twice under multiple interactions with the mid-latitude westerlies[1]. The system underwent rapid intensification within 24 hours. According to initial IMD forecasts, the system was expected to make landfall on the Gujrat coastline on 13 June, but the system recurved, skirting the Gujrat coastline further westwards under the influence of an anticyclonic circulation over the Arabian Peninsula region[1] .

The present study attempts to understand the synoptic features of this unique TC with the WRF-ARW model initiated with NCEP and GFS datasets with and without external SST data. The results indicated that the inclusion of SST data led to improved track estimates, especially at the recurving of the storm along the Gujrat coastline. Based on the track error estimates, another set of experiments is done where the model initiated with GFS data and external SST with fdda analysis grid nudging technique (referred to as WRF_GFS_SST_nud hereafter) led to a significant improvement in track estimates but with slight underestimations of wind speed intensity at the matured VSCS stage of the cyclone.

Given the improvement in cyclone trajectory with the nudging technique, further investigation of the storm's synoptic parameters and rapid intensification is conducted on simulations of WRF_GFS_SST_nud. Results show the positive impact of SST input and nudging technique into the simulations with a low overall mean track and intensity deviation of 26.44 km 1.64 m/s, respectively. The current model setup could skillfully capture the unique steering of the storm at the intensified stage on 16 June onwards with a slight track deviation of approximately 50 km, but the storm's weakening was well captured.

Model simulations could satisfactorily capture the storm intensification with anomalously high mid-tropospheric RH (%), low-level relative vorticity and low vertical wind shear, high SST(~ 31.5 °C), and other related synoptic parameters of the cyclone. Overall comparison of wind intensity during the storm with reanalysis data ERA-5indicates that the model simulates a stronger TC with a well-defined eyewall with increasing wind speed (30-40 m/s) from the outer to the inner wall matured VSCS stage of the storm. The skillful capture of high RH (%) (>90%) at the mid-troposphere at the initiation stage indicates favorable conditions for the onset of RI. The simulated storm shows a temperature anomaly of 4-6 k with a warm core favoring intensification on 12 June at 00 UTC. The model's mid-tropospheric thermal instability and that of ERA-5 data depict a rapidly intensifying warm core from the developing stage. Spatial distribution of vertical wind speed shear (m/s) WVS indicates low WVS collocated with the location of the storm center during various stages of the cyclone. The simulated storm shows a strong low level (850 hPa) relative vorticity indicating rapid intensification. However, compared to ERA-5, there exists a disparity in the location of the vorticity center on 13 June, an aspect which needs further investigation of the well known reanalysis data. The spatial distribution of simulated SST overlaid with SSHA contours and observed storm track indicates higher SST collocated with positive SSHA (10-20 cm), indicating higher upper ocean heat content. The simulated storm was found to have an

ACE of approximately 9.35×10^4 knts^{2,} while that of the observed is 11.54×10^4 knts^2 over the lifecycle of the cyclone, which is due to the underestimation of surface wind intensity at the matured VSCS stage which was seen all the datasets, indicating the major challenge in numerical forecasting in the data-scarce Arabian Sea. Overall, the results indicate the model's credibility with the current set of parameterizations with the analysis nudging technique can skillfully capture the synoptic features, track, and intensity of this unique TC of the Arabian sea.

Although the results show the skillful nature of the model setup to capture all the essential synoptic features of the storm, the inclusion of sophisticated data assimilation techniques might lead to even more improved track error estimates, which is considered a future scope of the study. A recent study by Krishnan *et al*.[72] indicated that SST and the upper ocean heat content of the Indian Ocean are increasing in the climate change scenarios; moreover, the climate change models predict a continued increase in SST[73], indicating more of such rapid intensifications with unique tracks in the Arabian Sea. Hence it is imperative to closely monitor the basin and understand the credibility of numerical models like WRF in simulating the track, intensity, and synoptic features of such TCs.

Competing Interests

The authors declare no competing financial interest

References

1 Mishra K, Sharma M & Mohapatra M, *J Earth Syst Sci,* 130 (2021) 1.
2 Mohapatra M, Mandal G S, Bandyopadhyay B K, Tyagi A & Mohanty U C, *Nat Hazards*, 63 (2012) 1601.
3 Mohapatra M & Sharma M, *Mausam*, 70 (2019) 635.
4 View of Comparative performance of HWRF model coupled with POM and HYCOM for tropical cyclones over North Indian Ocean. Available at: https://mausamjournal.imd.gov.in/index.php/MAUSAM/article/view/127/94. (Accessed: 17th March 2022).
5 View of Understanding the rapid intensification of tropical cyclone Titli using Hurricane WRF model simulations. Available at: https://mausamjournal.imd.gov.in/index.php/MAUSAM/article/view/129/97. (Accessed: 16th March 2022).
6 Nadimpalli R, Osuri K K, Pattanayak S, Mohanty U C, Nageswararao M M & Prasad S K, *Nat. Hazards*, 81 (2016) 1771.
7 Osuri K K, Mohanty U C, Routray A, Kulkarni M A & Mohapatra M, *Nat Hazards*, 63 (2012) 1337.
8 Osuri K K, Mohanty U C, Routray A, Kulkarni M A & Mohapatra M, *Int J Remote Sens,* 33 (2012) 1627.
9 Osuri K K, Mohanty U C, Routray A & Niyogi D, *Mon Weath*er *Rev*, 143 (2015) 4533.
10 Routray A, Mohanty U C, Osuri K K, Kar S C & Niyogi D, *IEEE Trans Geosci Remote Sens,* 54 (2016) 2285.
11 Osuri K K, Mohanty U C, Routray A, Mohapatra M & Niyogi D, *J Appl Meteorol Climatol*, 52 (2013) 2476.
12 Lakshmi D D, *et al.*, *Ocean Eng*, 131 (2017) 135.
13 Mohanty U C, Nadimpalli R, Mohanty S & Osuri K K, *Mausam*, 70 (2019) 57.
14 Munsi A, *et al., Atmos Res*, 259 (2021) 105678.
15 Lee H S, Yamashita T, Hsu J R C & Ding F, *Dyn Atmos Ocean,* 59 (2013) 1.
16 Liu P, Tsimpidi A P, Hu Y, Stone B, Russell A G & Nenes A, *Atmos Chem Phys*, 12 (2012) 3601.
17 Zittis G, Bruggeman A, Hadjinicolaou P, Camera C & Lelieveld J, *Atmosphere (Basel),* 9 (2018).
18 Spero T L, Otte M J, Bowden J H & Nolte C G, *Nature*, 175 (1955) 238.
19 Otte T L, Nolte C G, Otte M J & Bowden J H, *J Clim*, 25 (2012) 7046.
20 Bowden J H, Otte T L, Nolte C G & Otte M J, *J Clim*, 25 (2012) 2805.
21 Omrani H, Drobinski P & Dubos T, *Clim Dyn*, 41 (2013) 2451.
22 Bullock O R, Alapaty K, Herwehe J A, Mallard M S, Otte T L, Gilliam R C & Nolte C G, *J Appl Meteorol Climatol*, 53 (2014) 20.
23 Cione J J & Uhlhorn E W, *Mon Weather Rev*, 131 (2003) 1783.
24 Emanuel K, DesAutels C, Holloway C & Korty R, *J Atmos Sci*, 61 (2004) 843.
25 Trenberth K E & Shea D J, *Geophys Res Lett,* 33 (2006) 1.
26 Emanuel K, *Nature*, 436 (2005) 686.
27 Webster P J, Holland G J, Curry J A & Chang H R, *Science,* 309 (2005) 1844.
28 Sriver R & Huber M, *Geophys Res Lett,* 33 (2006) 1.
29 Vecchi G A & Soden B J, *Nature,* 450 (2007) 1066.
30 Powers J G, *et al. Bull Am Meteorol Soc,* 98 (2017) 1717.
31 Mielikainen J, Huang B, Huang H L A & Goldberg M D, *IEEE J Sel Top Appl Earth Obs Remote Sens,* 5 (2012) 1256.
32 Mielikainen J, Huang B, Huang H L A & Goldberg M D, *IEEE J Sel Top Appl Earth Obs Remote Sens*, 5 (2012) 555.
33 Huang M, Mielikainen J, Huang B, Chen H, Huang H L A & Goldberg M D, *Geosci Model Dev*, 8 (2015) 2977.
34 Thiebaux J, Rogers E, Wang W & Katz B, *Bull Am Meteorol Soc*, 84 (2003) 645.
35 Routray A, Mohanty U C, Niyogi D, Rizvi S R H & Osuri K K, *Meteorol Atmos Phys,* 106 (2010) 107.
36 Nadimpalli R, Osuri K K, Mohanty U C, Das A K, Kumar A, Sil S & Niyogi D, *Meteorol Atmos Phys*, 132 (2020) 1.
37 Richard A, *Bost. Am. Meteorol. Soc.* 19 (1982) 1.
38 Cangialosi J P & Franklin J L, *National Hurricane Center Forecast Verification Report*, (2014).
39 Hersbach H, *et al., Q J R Meteorol Soc*, 146 (2020) 1999.
40 Mandal S, Sil S, Shee A, Swain D & Pandey P C, *IEEE J Sel Top Appl Earth Obs Remote Sens*, 11 (2018) 845.
41 Figa J & Stoffelen A, *IEEE Trans Geosci Remote Sens*, 38 (2000) 1893.
42 Bentamy A, Grodsky S A, Carton J A, Croizé-Fillon D & Chapron B, *J Geophys Res Ocean,* 117 (2012) 1.
43 Chakraborty A, Kumar R & Stoffelen A, *Remote Sens Lett*, 4 (2013) 84.

44 Singh S K, Singh R, Singh C & Singh R, *Meteorol Atmos Phys*, 134 (2022) 1.

45 Cyclone Warning In India Standard Operation Procedure India Meteorological Department Ministry of Earth Sciences Government of India INSAT 3D-18/0300 UTC India Meteorological Department Ministry of Earth Sciences Ministry of Earth Sciences Government of India, PREFACE, (2021).

46 Judt F & Chen S S, *Mon Weather Rev*, 144 (2016) 4395.

47 Mohanty U C, Nadimpalli R & Mohanty S, *Mausam*, 72 (2021) 167.

48 Hodges K, Cobb A & Vidale P L, *J Clim*, 30 (2017) 5243.

49 Subrahamanyam D B, Ramachandran R, Nalini K, Paul F P & Roshny S, *Natural Hazards*, 96 (2019) 431.

50 Jaiswal N, Kumar P & Kishtawal C M, *Curr Sci,* 117 (2019) 983.

51 Wu L, *et al*., *Geophys Res Lett,* 39 (2012) 1.

52 Ramakrishna S S V S, *et al., Pure Appl Geophys*, 176 (2019) 5445.

53 Kotal S D, Kundu P K & Bhowmik R S K, *Nat Hazards*, 50 (2009) 389.

54 Ganesh S S, Sahai A K, Abhilash S, Joseph S, Kaur M & Phani R, *Adv Earth Space Sci*, 7 (2020) 1.

55 Paterson L A, Hanstrum B N, Davidson N E & Weber H C, *Mon Weather Rev*, 133 (2005) 3644.

56 Chih C H & Wu C C, *J Clim*, 33 (2020) 1031.

57 Balaguru K, *et al.*, *Geophys Res Lett*, 49 (2022) 1.

58 Singh V, Srivastava A K, Samanta R, Singh A, Kumar A & Singh A K, *Indian J Pure Appl Phys*, 61 (2023) 175.

59 Klotzbach P J, *J Clim*, 27 (2014) 2317.

60 Kotal S D, Kundu P K & Roy B S K, *Nat Hazards*, 50 (2009) 389.

61 Kotal S B, *Mausam*, 64 (2013) 149.

62 Lin I I, Goni G J, Knaff J A, Forbes C & Ali M M, *Nat Hazards*, 66 (2013) 1481.

63 Goni G J & Trinanes J A, *Adv Earth Space Sci*, 84 (2003) 573.

64 Shay L K & Brewster J K, *Mon Weather Rev*, 138 (2010) 2110.

65 Gospalan A K S, Gopala K V V, Ali M M & Sharma R, *J Mar Res*, 58 (2000) 721.

66 Ali M M & Jain S, *Satellite Altimetry for Indian Ocean Studies*, (2006).

67 Bhowmick S A, *et al.*, *Curr Sci*, 119 (2020) 1510.

68 Trugman A T, *et al., J Adv Model Earth Syst*, 8 (2016) 1180.

69 Pun I F, Lin I I, Lien C C & Wu C C, *Mon Weather Rev*, 146 (2018). 661.

70 Singh V K, Roxy M K & Deshpande M, *Curr Sci,* 119 (2020).

71 Balaji M, Chakraborty A & Mandal M, *Int J Climatol*, 38 (2018) 2819.

72 Krishnan R, *et al., Assessment of Climate Change over the Indian Region: A Report of the Ministry of Earth Sciences (MoES), Government of India* (2020).

73 Terry J, Al R A, Boldi R, Gienko G & Stahl H, *Weather*, (2022) 1.